Device Modeling of Graded III-N HEMTs for Improved Linearity

M.G. Ancona
Electronics S&T Division
Naval Research Laboratory
Washington, DC, USA
mario.ancona@nrl.navy.mil

J.P. Calame
Electronics S&T Division
Naval Research Laboratory
Washington, DC, USA
jeff.calame@nrl.navy.mil

D.J. Meyer
Electronics S&T Division
Naval Research Laboratory
Washington, DC, USA
dave.meyer@nrl.navy.mil

S. Rajan
Electrical & Comp. Engineering
The Ohio State University
Columbus, OH, USA
rajan@ece.osu.edu

***Abstract*—When GaN HEMTs are used in power amplifier applications, their performance falls well short of ideal due to power-gain roll-off that results from having a peaked transconductance characteristic. A promising design solution involves compositionally grading the channel, and we here formulate a numerical device model to explore this approach that couples linear electroelasticity, diffusion-drift transport with new mobility models, and density-gradient theory. Lumped modeling of the large-signal behavior is also developed to explore the power amplifier performance. Preliminary results presented here indicate that the graded-channel idea has value, especially for gate lengths greater than about 100nm.**

Keywords—GaN HEMTs, linearity, compositional grading, transport modeling, RF power amplifier.

I. Introduction

The III-N material system has received much attention for power amplifiers because of its promising combination of high electron velocity and high breakdown voltage, and important technological progress has been made. However, the full promise of these materials has yet to be realized for various reasons [1]. Our interest here is in premature degradation of linearity that is frequently seen at high RF power, and on the possibility that it may be mitigated by compositional grading of the HEMT channel [2].

It is quite challenging to fabricate a graded-channel III-N HEMT with precise control over the compositional variation and including a sufficiently short gate, regrown contacts, and other features commonly used in GaN technology. For this reason, the situation is one for which numerical device simulation can be quite valuable as a tool for understanding the device concept, evaluating its merit, and proposing optimal designs as targets for fabrication. To this end, it is essential that the modeling incorporate all of the potentially important device physics. This includes the piezoelectric nature of the III-N materials and especially of their inhomogeneous alloys, mobility models that for example incorporate effects of alloy scattering and the dependence of the saturation velocity on density [2], quantum confinement effects, etc. In this paper, we formulate such a model and then demonstrate its use with an initial exploration of various compositionally-graded III-N HEMT designs.

The authors thank the Office of Naval Research for funding support, and S.R. acknowledges funding through ONR Grant N00014-15-1-2363 managed by Dr. Paul Maki.

II. Modeling Methods

A. Device Modeling

In order to investigate compositionally-graded III-N HEMTs we create a device description that couples three types of continuum models that have not been joined heretofore. These models are detailed next.

To describe the piezoelectric nature of the III-N materials, including with compositional grading, we employ linear electroelasticity [3] with the key equations being the material response functions:

$$\tau_a = \tau_a^0 + c_{ab} S_b + e_{ka} \psi_{,k} \qquad (1a)$$

$$D_i = P_i^0 + e_{ia} S_a - \varepsilon_{ik} \psi_{,k} \qquad (1b)$$

where τ_a is the stress tensor, D_i is the electric displacement vector, indices *i* and *k* vary over the component directions (*x*, *y*, and *z*), *a* and *b* vary over the six component pairs *xx*, *yy*, *zz*, *yz/zy*, *xz/zx*, and *xy/yx*, and the Einstein summation convention is assumed. Also, ψ is the electric potential, S_a is the linear strain tensor, τ_a^0 is the built-in stress, P_i^0 is the spontaneous polarization, and c_{ab}, e_{ia}, and ε_{ik} are tensors containing the elastic, piezoelectric, and dielectric constants, respectively. The values assumed for all of these material coefficients are the same as in [3].

The main equation of the electron transport description is the diffusion-drift current equation for electrons:

$$J_i^n = q n \mu_n [\varphi_n^{DD}(n) - \psi]_{,i} \qquad (2)$$

where the chemical potential function $\varphi_n^{DD}(n)$ prescribes the equation of state for the electron gas. For accurate modeling, the most important quantity to have well calibrated is the electron mobility μ_n, which can in principle have functional dependences on any of the field variables. In this regard, both low-field and high-field behaviors need to be considered, with functional forms chosen, and parameters estimated by fitting appropriate experimental data. Here, we use characterization data obtained in [2] for *non-graded* GaN channels. For low fields, experiment (Fig. 1A, points) finds that the mobility rises with increased sheet density, and a reasonable assumption is that this is caused by screening of Coulombic and/or dislocation scattering. A low-field mobility model capable of capturing this effect is:

$$\mu_n^{LF} = \frac{\mu_n^b}{1 + \frac{\mu_n^b}{\mu_n^c} \exp\left(-\frac{z}{z_c}\left[1 + \left(\frac{D_z^{bulk} - D_z^{surf}}{\varepsilon_s E_c}\right)^{\alpha_c}\right]\right)} \quad (3)$$

where the exponential quantifies the dependence of the screening on distance z from the surface and on channel density (via the electric displacement). Choosing the parameters $\mu_n^b = 1700cm^2/Vs$, $\mu_n^c = 50cm^2/Vs$, $\alpha_c = 3$, $z_c = 18nm$, and $E_c = 260kV/cm$, we obtain the fit to the data of [2] shown in Fig. 1A.

Regarding mobility under high field conditions, this aspect is especially important for us because it has previously been implicated as a cause for the premature onset of nonlinearity in GaN HEMTs [2]. In particular, the roll-off was ascribed to a drop in electron saturation velocity at high channel density (Fig. 1B, points) that was said to result from stimulated LO phonon emission [2] (or possibly surface roughness scattering [4]). On this basis, we assume the velocity saturation model:

$$\mu_n = \frac{\mu_n^{LF}}{\left[1 + \left(\frac{\mu_n^{LF}|\phi_x^n|}{v_{sat}}\right)^{\beta_s}\right]^{\frac{1}{\beta_s}}} \quad v_{sat} = \frac{v_{sat}^0}{\left[1 + \left(\frac{\alpha_v n}{n + n_v}\right)^{\beta_v}\right]^{\frac{1}{\beta_v}}} \quad (4)$$

where ϕ^n is the electron quasi-Fermi level and the dependence of v_{sat} on n causes it to drop as the channel density rises. Using (4) in a simulation at high drain bias allows the experiment of Fig. 1B to be modeled, and as seen in the figure a reasonable fit is obtained if $v_{sat}^0 = 2.3x10^7 cm/s$, $n_v = 2x10^{17}cm^{-3}$, $\beta_s = 1$, $\beta_v = 2.5$, and $\alpha_v = 3.2$.

Given our interest in the carrier density profile across the channel and its effect on device linearity, we decided to include explicitly the effect on that profile imposed by quantum confinement near the HEMT barrier. For this purpose, we use the density-gradient (DG) approach [5] in which the chemical potential of (2) is generalized to include a gradient term. For highest accuracy, we fit quantum mechanical solutions using a DG effective mass [5]. Also, in applying DG theory, it is important to be careful in treating the ohmic contact conditions as was discussed in [6].

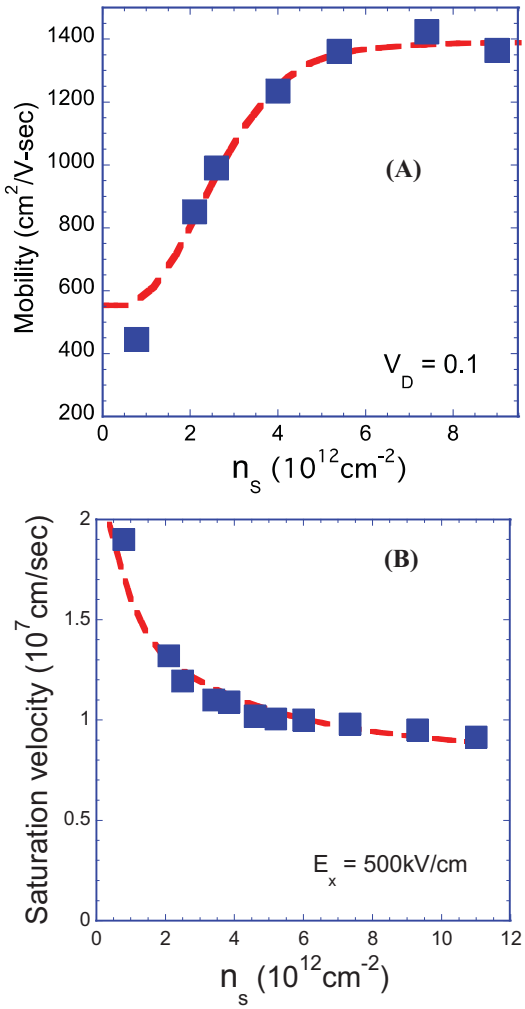

Fig. 1. Experimental (points) [4] versus simulated (lines) (A) low-field mobility and (B) saturation velocity at high V_{DS}.

B. Nonlinear Response Modeling

The equations of the previous sub-section define a partial differential system that allow a GaN HEMT design and its dc electrical characteristics $I_D(V_G, V_D)$ to be simulated. To treat

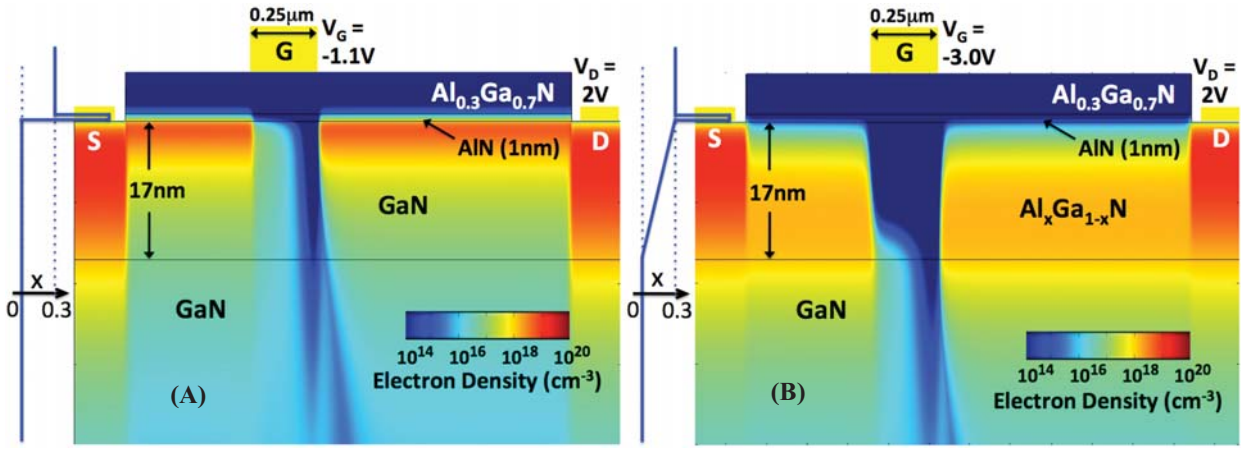

Fig. 2. Contour plots of electron density for (A) ungraded and (B) graded devices at gate bias near pinch-off.

such devices under the large-signal ac conditions of an operating power amplifier the model must be supplemented with descriptions of various extrinsic aspects like the input/output matching circuitry and parasitics. Because our focus is on intrinsic effects, we do not carry out this full simulation program, and instead emphasize two cruder measures of the large-signal ac performance that can provide a useful initial screening. The first judges the device design based simply on the "flatness" of its $g_m(V_G)$ curve, while the second employs the simulated $I_D(V_G)$ at a large V_D to approximate the saturated transfer function in a circuit simulator. Time-domain simulations are then used to model the nonlinear response to a single tone or two tones.

C. Numerical Methods

To perform the continuum device simulations, we employ the convenient computational framework provided by COMSOL [7]. This finite element package greatly facilitates the generation and meshing of the geometry, and the flexible handling of the discretization and solution of the governing equations. The time-domain circuit simulations of the nonlinear response are carried out with a C++ code in Visual Studio.

III. Results

We first consider two 0.25μm HEMTs having the heterostructure design $Al_{0.3}Ga_{0.7}N(5nm)/AlN(1nm)/Al_xGa_{1-x}N$ (17nm)/GaN, and with either no grading (x = 0) or a linear grading down from x_{max} = 0.3 [2]. Contour plots of the electron densities for a bias near pinchoff are shown in Figs. 2A,B and the profiles across the channel as a function of V_G are shown in Figs. 3A,B. The graded channel is seen to deplete out from the surface, and maintain a much lower and nearly

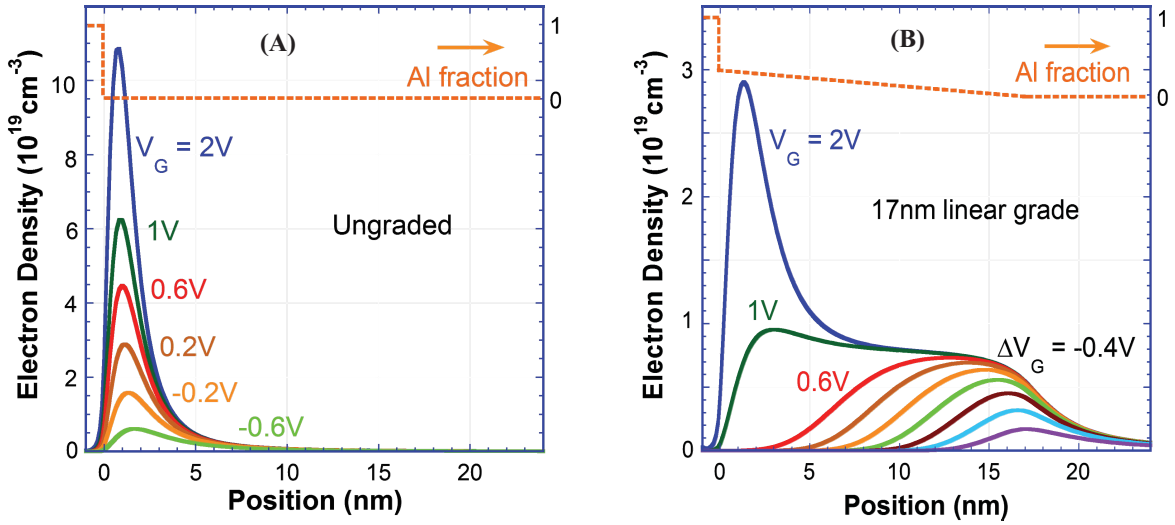

Fig. 3. Density profiles in the (A) ungraded and (B) graded devices as a function of gate bias.

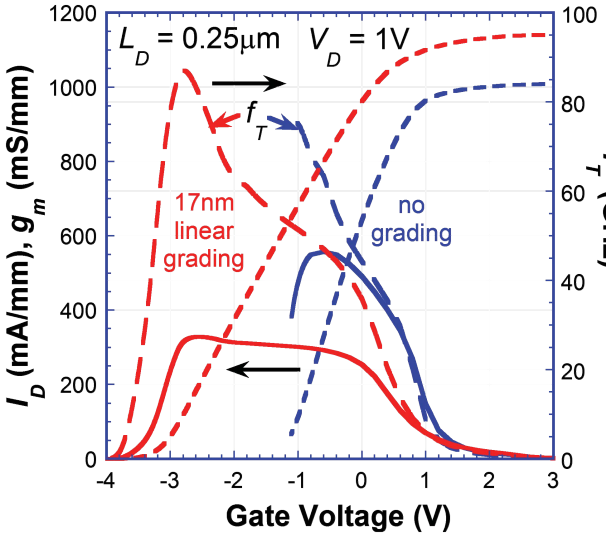

Fig. 4. I_D, g_m, and f_T versus V_G for the ungraqded and graded devices.

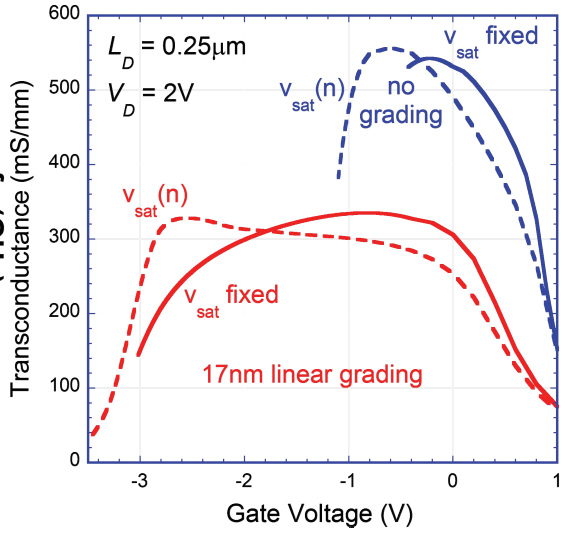

Fig. 5. g_m for ungraded and graded HEMTs with v_{sat} constant or a function of n.

constant volumetric density over a wide range of biases thus acting to keep v_{sat} high [2]. Comparisons of the simulated transfer curves, g_m, and f_T (Fig. 5) for the two devices find the graded device to have a lower and much flatter g_m, and so better linearity is expected. Looking closer at the graded device, in Fig. 5 we compare g_m (normalized) values with results if v_{sat} is fixed at 1.2x10^{7}cm/sec. Clearly the graded device gives a flatter g_m even for constant v_{sat}, suggesting a depletion mechanism like that discussed in [8] is more important than the v_{sat} effect. Following this idea further, [8] showed that the doping profile shape can be used to tailor the depletion and improve linearity, and a similar strategy can be pursued using composition. In particular, we round the composition profile taking $x = x_{max}\{1 - \tanh^{1/\beta}[(y/17nm)^{\beta}]\}$, and find g_m and its flatness can be significantly improved (Fig. 6). The benefit is further probed in lumped simulations of the gain compression in response to a single tone (Fig. 7A), and in a two-tone simulation of the 3rd-order intermodulation products (with one shown in Fig. 7B). By all metrics, the $\beta = 1.5$ design is seen to be by far the best. A potential drawback of compositionally graded HEMTs is their scaling behavior. In Fig. 8 we plot the V_T shift and the drain-induced barrier lowering ($DIBL$) versus L_G for a 17nm graded design, and clearly observe the onset of substantial short channel effects that suggest the compositional grading approach to improving linearity will be limited to $L_G \geq 100nm$.

IV. Final Remarks

We have formuated a numerical device model to explore the use of compositional grading for flattening the transconductance characteristic of GaN HEMTs in order to reduce power-gain roll-off. The model couples equations of linear electroelasticity, diffusion-drift transport, and density-gradient theory. Through these simulations as well as lumped modeling of the large-signal behavior we find promise in the graded-channel idea, especially for gate lengths greater than about 100nm.

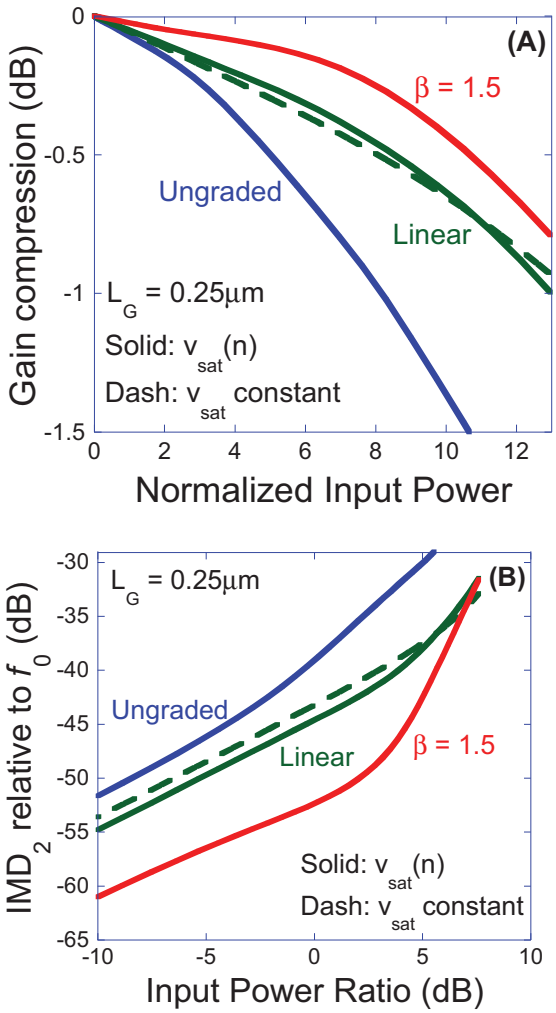

Fig. 7. Shown for various HEMT compositional gradings: (A) gain compression when normalized so that unity input power on the abscissa produces 0.8W/mm output power, (B) second intermod product for two tones with the 2nd signal at 1.083 times higher frequency.

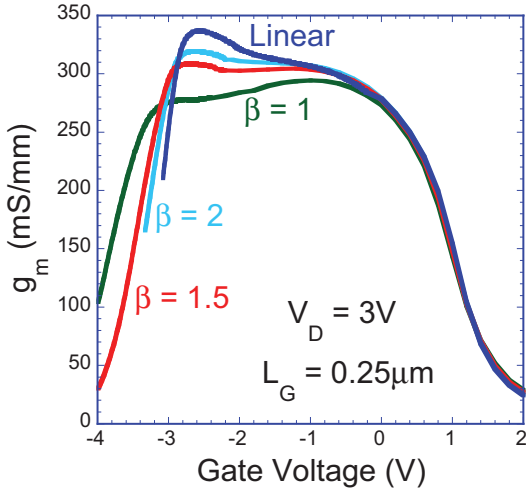

Fig. 6. Transconductance for the various graded devices.

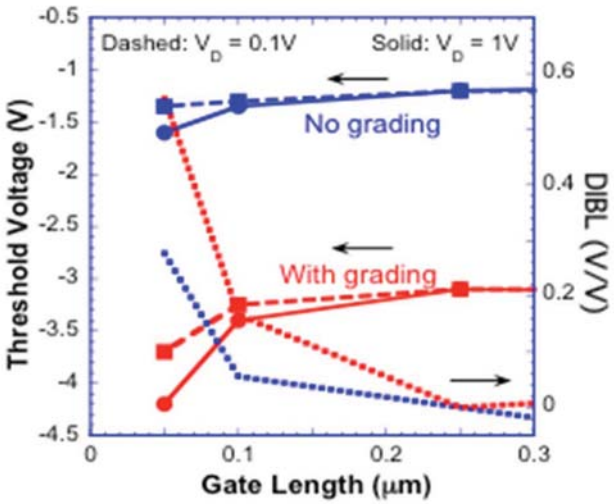

Fig. 8. Threshold voltage shift and DIBL versus gate length.

REFERENCES

[1] C.-H. Chen *et al.,* "The causes of GaN HEMT bell-shaped transconductance degradation," *Solid-St. Elect.* 126, 115 (2016).

[2] S. Bajaj, Z. Yang, F. Akyol, P.S. Park, Y. Zhang, A.L. Price, S. Krishnamoorthy, D.J. Meyer, and S. Rajan, "Graded AlGaN channel transistors for improved current and power gain linearity," *IEEE Trans. Elect. Dev.* **64**, 3114 (2017).

[3] M.G. Ancona, S.C. Binari, and D.J. Meyer, "Fully coupled thermoelectromechanical analysis of GaN HEMT degradation," *J. Appl. Phys.* **111**, 074504 (2012).

[4] J.R. Juang, T.-Y. Huang, T.-M. Chen, M.-G. Lin, G.-H. Kim, Y. Lee, C.T. Liang, D.R. Hang, Y.F. Chen, and J.-I. Chyi, "Transport in a gated AlGaN-GaN electron system," *J. Appl. Phys.*, 94 (2003).

[5] M.G. Ancona, "Density-gradient theory: A macroscopic approach to quantum confinement and tunneling in semiconductor devices," *J. Comp. Elec.* **10**, 65 (2011).

[6] M.G. Ancona, D. Yergeau, Z. Yu, and B.A. Biegel, "On ohmic boundary conditions for density-gradient theory," *J. Comp. Elect.* **1**, 103 (2002).

[7] See www.comsol.com.

[8] R.E. Williams and D.W. Shaw, "Graded channel FETs: Improved linearity and noise figure," *IEEE Trans. Elect. Dev.* **25**, 600 (1978).